

Supplemental material for “Generalized Efimov scenario for heavy-light mixtures”

D. Blume and Yangqian Yan¹

¹*Department of Physics and Astronomy, Washington State University, Pullman, Washington 99164-2814, USA*

(Dated: August 22, 2014)

The notation employed in this supplemental material follows that introduced in the main text.

PACS numbers:

BASIS SET EXPANSION APPROACH

To solve the time-independent Schrödinger equation for the Hamiltonian H given in Eq. (1) of the main text, we employ an explicitly correlated Gaussian basis set [1, 2]. The eigenfunctions ψ_β of the Hamiltonian H are expanded in terms of the basis functions $\phi_l^{(\beta)}$,

$$\psi_\beta = \sum_{l=1}^{N_b} c_l^{(\beta)} \phi_l^{(\beta)}, \quad (1)$$

where each of the basis functions $\phi_l^{(\beta)}$,

$$\phi_l^{(\beta)} = \mathcal{S} \exp \left[-\frac{1}{2} \sum_{j=1}^{N-1} \sum_{k>j}^N \left(\frac{r_{jk}}{\alpha_{jk}^{(l)}} \right)^2 \right], \quad (2)$$

depends on $N(N-1)/2$ independent non-linear variational parameters $\alpha_{jk}^{(l)}$ that are optimized semi-stochastically. For notational simplicity, the dependence of the $\alpha_{jk}^{(l)}$'s on the state index β is not indicated explicitly in Eq. (2). \mathcal{S} denotes a symmetrizer that ensures that the basis function $\phi_l^{(\beta)}$ is symmetric under the exchange of any two identical bosons. The $c_l^{(\beta)}$ denote linear variational or expansion parameters that are determined by solving the generalized eigenvalue problem $\underline{H}\underline{c}^{(\beta)} = E_\beta^{\text{var}} \underline{Q}\underline{c}^{(\beta)}$, where \underline{H} and \underline{Q} denote the Hamiltonian and (non-diagonal) overlap matrices, respectively. The vector $\underline{c}^{(\beta)}$ contains the coefficients $c_1^{(\beta)}, \dots, c_{N_b}^{(\beta)}$, where N_b denotes the size of the matrix (or equivalently, the size of the basis set). According to the variational principle, the energies E_β^{var} are upper bounds to the exact eigenenergies E_β . Assuming that $E_1^{\text{var}} \leq E_2^{\text{var}} \leq \dots \leq E_{N_b}^{\text{var}}$, one has $E_1 \leq E_1^{\text{var}}, E_2 \leq E_2^{\text{var}}, \dots$. The matrix elements $H_{ll'}$ and $O_{ll'}$ have closed analytical expressions and the generalized eigenvalue problem is solved using one of ARPACK's eigenvalue solvers.

The superscript “ (β) ” on the right hand side of Eq. (1) indicates that the basis set is constructed for the β th eigenstate ψ_β . While one could construct a single basis set that provides a good description of the lowest few eigenstates, our work takes advantage of the fact that the basis set can be optimized separately for each eigenstate. For the BBX system, e.g., the two energetically lowest-lying states differ in size by the scaling factor λ . This

implies that the variational parameters $\alpha_{jk}^{(l)}$ that yield an efficient description of the ground state (the state with $\beta = 1$) and of the first excited state (the state with $\beta = 2$) are very different. Another key point of the basis set expansion approach is that the basis set can be systematically improved. Our three-body energies are, except very close to the three-atom break-up threshold, converged to 0.1% or better. Our four-body energies are converged to 1% or better. For the B_3X system at unitarity with $\kappa = 133/6$, e.g., we clearly see that the energy of the first excited four-body state lies below that of the lowest BBX state.

BENCHMARKING OUR APPROACH: N IDENTICAL BOSONS

To validate our approach, we consider N identical bosons of mass m_B with infinitely large s -wave scattering length a_s described by the Hamiltonian H_B ,

$$H_B = \sum_{j=1}^N -\frac{\hbar^2}{2m_B} \nabla_{\vec{r}_j}^2 + V_{2b} + V_{3b}. \quad (3)$$

The potential V_{2b} accounts for the interactions between all $N(N-1)/2$ pairs,

$$V_{2b} = \sum_{j=1}^{N-1} \sum_{k>j}^N v_0 \exp \left(-\frac{r_{jk}^2}{2r_0^2} \right), \quad (4)$$

where v_0 and r_0 denote the depth and range of the attractive two-body Gaussian. The depth and range are adjusted such that the free-space two-body system supports one zero-energy bound state. The potential V_{3b} accounts for the interactions between all $N(N-1)(N-2)/6$ triples,

$$V_{3b} = \sum_{j=1}^{N-2} \sum_{k>j}^{N-1} \sum_{l>k}^N V_0 \exp \left(-\frac{r_{jk}^2 + r_{kl}^2 + r_{lj}^2}{2R_0^2} \right), \quad (5)$$

where V_0 and R_0 denote the depth and range of the repulsive three-body Gaussian. Our calculations use $R_0 = \sqrt{8}r_0$. As discussed in Ref. [3], the repulsive three-body potential serves to eliminate deeply-bound non-universal states in the $N = 3$ sector. In essence, the three-body potential “cuts off” the short-range portion of the effective hyperradial potential curve that is

governed by the two-body effective range and deviates from the effective three-body hyperradial Efimov potential curve. Using this model, the ratio of the binding momenta of the two energetically lowest-lying three-body states is $(E_3^{(1)}/E_3^{(2)})^{1/2} = 22.99$ for $V_0 = 0$, takes a minimum value of $(E_3^{(1)}/E_3^{(2)})^{1/2} = 21.48$ for $V_0 \approx 0.3E_{\text{sr}}$, and approaches $(E_3^{(1)}/E_3^{(2)})^{1/2} = 22.71$ as $V_0 \rightarrow \infty$. For $V_0 \geq E_{\text{sr}}$, the ratio $E_3^{(1)}/E_3^{(2)}$ lies within 0.08% of the universal zero-range value of 22.694. The small difference of the binding momentum ratios for the finite-range Hamiltonian H_{B} and for the zero-range model can be attributed to the fact that both $V_{2\text{b}}$ and $V_{3\text{b}}$ have a finite range.

The four identical boson system with infinitely large s -wave scattering length has been benchmarked most precisely by Deltuva [4] using a momentum space representation that allows for the treatment of bound and resonance states. It was shown that the four-body energies $E_4^{(n,1)}$ and $E_4^{(n,2)}$ approach the ratios $(E_4^{(n,1)}/E_3^{(n)})^{1/2} = 2.147$ and $(E_4^{(n,2)}/E_3^{(n)})^{1/2} = 1.0011$, respectively, for sufficiently large n [4]. For the Hamiltonian given in Eq. (3) with $V_0 = 4.8E_{\text{sr}}$, we find (see also the main text) that the binding momentum ratio of the lowest four-body state and the lowest three-body state is $(E_4^{(1,1)}/E_3^{(1)})^{1/2} = 2.127(5)$. For this V_0 , the lowest three-body energy is $-2.64 \times 10^{-4}E_{\text{sr}}$, i.e., the three-body system is large compared to both r_0 and R_0 and thus, to a good approximation, independent of r_0 and R_0 . We also find a weakly-bound excited four-body state with the binding momentum ratio $(E_4^{(1,2)}/E_3^{(1)})^{1/2} \geq 1.0004$ that is tied to the lowest three-body state. Although the variational principle does not apply to energy ratios, we can assign the “ \geq ” sign since the energy of the lowest three-body state has a significantly smaller basis set error than the energy of the excited four-body state.

HEAVY-LIGHT (2, 1) SYSTEM AT UNITARITY

To validate our calculations for the (2, 1) system with unequal masses, we consider the case where the interspecies s -wave scattering length is infinitely large and the intraspecies two-body potential is set to zero. In the limit of zero-range interactions, the hyperangular and hyperradial degrees of freedom separate, and the hyperradial density $P_{\text{hyper}}(R)$ can be calculated analytically [5] (see the solid line in Fig. 1 for $\kappa = 133/6$). Here, the hyper-radius R is defined through

$$\mu R^2 = \sum_{j=1}^2 m_{\text{B}}(\vec{r}_j - \vec{r}_{\text{cm}})^2 + m_{\text{X}}(\vec{r}_3 - \vec{r}_{\text{cm}})^2, \quad (6)$$

where \vec{r}_{cm} denotes the center-of-mass vector of the B_2X system. For comparison, squares and circles show the hyperradial densities for the energetically lowest-lying

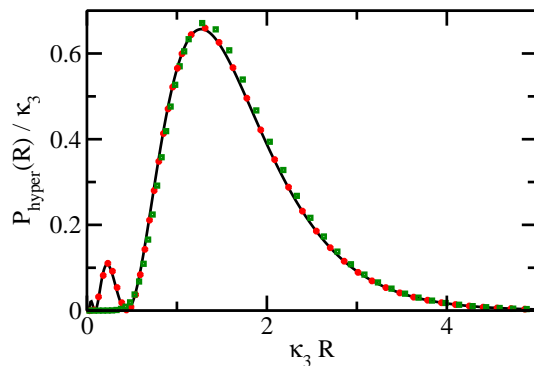


FIG. 1: (Color online) Hyperradial density $P_{\text{hyper}}(R)$ for the B_2X system with infinitely large interspecies s -wave scattering length and $\kappa = 133/6$. The squares and circles show the hyperradial densities for the ground and first excited state of the finite-range model Hamiltonian with $V_0 = 3.2E_{\text{sr}}$ and $R_0 = \sqrt{8}r_0$. The solid line shows the hyperradial density for the zero-range model Hamiltonian. For all three curves, dimensionless units are used (see the text for details).

and second lowest-lying states obtained from our basis set expansion calculations for the Hamiltonian H [see Eq. (1) of the main text]. To make this figure, the lengths have been scaled by the three-body parameter κ_3 . For the circles and the solid line, κ_3 is defined through $\hbar^2 \kappa_3^2 / (2\mu) = |E_3^{(2)}|$, where $E_3^{(2)}$ is the energy of the first excited state of the finite-range model Hamiltonian. For the squares, we define κ_3 through $\hbar^2 \kappa_3^2 / (2\mu) = \lambda^2 |E_3^{(2)}|$, where λ is obtained by solving the hyperangular portion of the zero-range model Hamiltonian. As shown in Table I of the main text, this zero-range scaling factor is very close to the scaling factor obtained from the spacing between the two lowest three-body energies of the finite-range model Hamiltonian. The good agreement for $\kappa_3 R \gtrsim 0.5$ between the hyperradial density for the zero-range model and the hyperradial densities of the finite-range Hamiltonian with two- and three-body interactions demonstrates that the model Hamiltonian employed in our work captures the Efimov physics in the three-body sector accurately.

Varying V_0 changes the three-body parameter. The scaled hyperradial densities and energy ratios, however, are, to a good approximation, unchanged for $V_0 \gtrsim E_{\text{sr}}$ and agree well with those for the zero-range model. As an example, Fig. 2 shows the binding momentum ratio $(E_3^{(1)}/E_3^{(2)})^{1/2}$ as a function of V_0 for infinitely large interspecies s -wave scattering length and $\kappa = 133/6$. As can be seen, the binding momentum ratio is approximately independent of V_0 for $V_0 \gtrsim E_{\text{sr}}$. In the large V_0 limit, the binding momentum ratio is close but not identical to the binding momentum ratio predicted by the zero-range theory. The small deviation can be attributed to the weak breaking of the discrete scale invariance of the

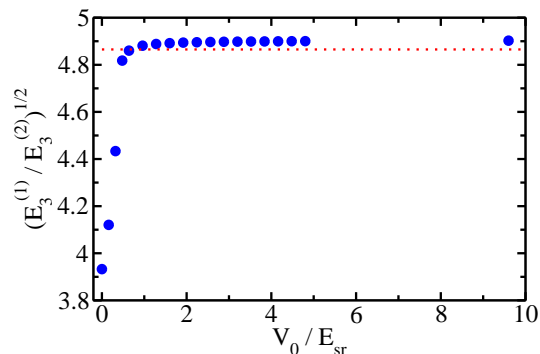


FIG. 2: (Color online) Symbols show the binding momentum ratio $(E_3^{(1)}/E_3^{(2)})^{1/2}$ as a function of V_0 for the B_2X system with infinitely large interspecies s -wave scattering length and $\kappa = 133/6$. For these calculations, we used $R_0 = \sqrt{8}r_0$. The dotted line shows the binding momentum ratio for the zero-range model.

model Hamiltonian by the finite-range two- and three-body interactions.

HEAVY-LIGHT (3,1) SYSTEM

Symbols in Figs. 3(a) and 3(b) show the binding momentum ratios $(E_4^{(1,1)}/E_3^{(1)})^{1/2}$ and $(E_4^{(1,2)}/E_3^{(1)})^{1/2}$, respectively, as a function of V_0 for infinitely large interspecies s -wave scattering length a_s , vanishing intraspecies interactions and $\kappa = 133/6$. The binding momentum ratios are approximately independent of V_0 for $V_0 \gtrsim E_{sr}$. This suggests that the properties of the B_3X system are, to a good approximation, determined by the two-body s -wave scattering length a_s and the three-body parameter κ_3 .

To further test the robustness of our results against changes of the parameters in the model Hamiltonian, we considered a 1.5 times larger range of the repulsive three-body potential while keeping the two-body range r_0 unchanged. The resulting change in the observables was found to be quite small. In addition, we varied the functional form of V_{3b} , i.e., we considered a repulsive three-body potential that is parameterized in terms of the hyperradii of the B_2X subsystems as opposed to the sum of the squares of the interparticle distances. The key difference between this alternative parametrization and the parametrization employed earlier is that this alternative three-body potential does, for the B_2X system, not depend on the hyperangles; note, however, that this alternative V_{3b} does depend on the hyperangles for $N \geq 4$. For this three-body potential, the four-body states are bound a bit more weakly relative to the lowest three-body state than for the three-body potential used in the main text. At unitarity, we obtain $(E_4^{(1,1)}/E_3^{(1)})^{1/2} = 1.47(2)$

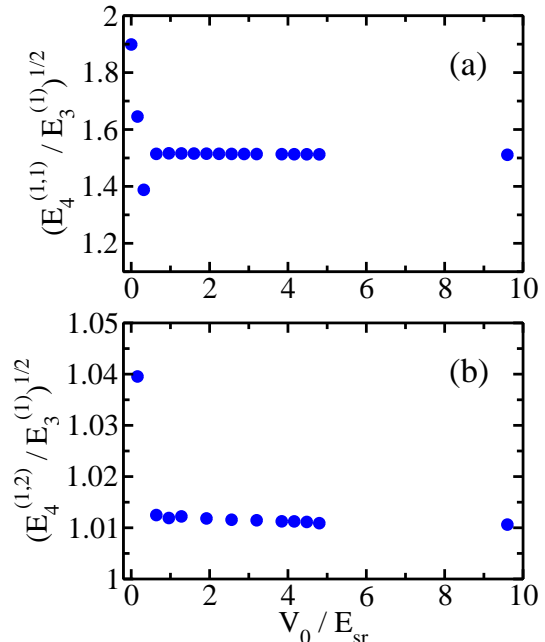


FIG. 3: (Color online) Symbols show the binding momentum ratios (a) $(E_4^{(1,1)}/E_3^{(1)})^{1/2}$ and (b) $(E_4^{(1,2)}/E_3^{(1)})^{1/2}$ as a function of V_0 for the heavy-light system with infinitely large interspecies s -wave scattering length and $\kappa = 133/6$. For these calculations, we used $R_0 = \sqrt{8}r_0$.

and $(E_4^{(1,2)}/E_3^{(1)})^{1/2} \geq 1.004$. For the scattering lengths at which the four-body system becomes unbound, we find $a_{4,-}^{(1,1)} \approx 0.57a_{3,-}^{(1)}$ and $a_{4,-}^{(1,2)} \approx 0.92a_{3,-}^{(1)}$. For comparison, the corresponding values reported in the main text are 0.55 and 0.91, respectively. The mass ratio at which the excited four-body state ceases to exist at unitarity changes from approximately 13 (this is the value reported in the main text) to 17 for the alternative three-body potential. These calculations suggest that the generalized Efimov scenario discussed in the main text is fairly robust with respect to changes in the model Hamiltonian.

-
- [1] Y. Suzuki and K. Varga, *Stochastic Variational Approach to Quantum Mechanical Few-Body Problems*, Springer Verlag, Berlin (1998).
 - [2] J. Mitroy, S. Bubin, W. Horiuchi, Y. Suzuki, L. Adamowicz, W. Cencek, K. Szalewicz, J. Komasa, D. Blume, and K. Varga, *Rev. Mod. Phys.* **85**, 693 (2013).
 - [3] J. von Stecher, *J. Phys. B* **43**, 101002 (2010).
 - [4] A. Deltuva, *Few-Body Systems* **54**, 569 (2013).
 - [5] E. Braaten and H.-W. Hammer, *Phys. Rep.* **428**, 259 (2006).